Acta Crystallographica Section D
Biological Crystallography
ISSN 0907-4449

Crystallization and preliminary X-ray crystallographic analysis of the excisionase–DNA complex from bacteriophage λ

My D. Sam,[a] Duilio Cascio,[a] Reid Johnson[b,c] and Robert T. Clubb[a,b]*

[a]Department of Chemistry and Biochemistry and the UCLA-DOE Center for Genomics and Proteomics, University of California, Los Angeles, 405 Hilgard Avenue, Los Angeles, CA 90095-1570, USA, [b]Molecular Biology Institute, University of California, Los Angeles, 405 Hilgard Avenue, Los Angeles, CA 90095, USA, and [c]Department of Biological Chemistry, UCLA School of Medicine, 10833 Le Conte Avenue, Los Angeles, CA 90095-1737, USA

Correspondence e-mail: rclubb@mbi.ucla.edu

Received 27 January 2003
Accepted 15 April 2003

Bacteriophage λ uses an elegantly regulated and highly directional site-specific DNA-recombination reaction to integrate and excise its genome. A critical regulator of this process is the phage-encoded excisionase (Xis) protein, which dramatically stimulates excision by orchestrating the assembly of a higher order nucleoprotein structure that excises the prophage. The Xis protein stabilizes this recombination intermediate by substantially altering the trajectory of viral DNA and by cooperatively interacting with the λ integrase (Int) protein. In an attempt to understand how Xis controls the directionality of bacteriophage λ recombination, co-crystals of the DNA-binding domain of Xis in complex with its binding site within the P-arm of the phage have been obtained using the hanging-drop vapor-diffusion method. Using sodium acetate as a precipitating reagent, the Xis–DNA complex crystallizes in space group *C*2, with unit-cell parameters $a = 80.2$, $b = 72.7$, $c = 38.8$ Å, $\beta = 104.1^\circ$. These crystals diffract beyond 1.5 Å resolution and are well suited for structural analysis using X-ray crystallography.

1. Introduction

A highly regulated and precise site-specific DNA-recombination reaction excises the genome of bacteriophage λ from the chromosome of its bacterial host (Azaro & Landy, 2002). The strand joining and cutting reactions of excision are performed by the phage-encoded integrase (Int) protein within the context of a higher order nucleoprotein complex called the excisive intasome. The phage-encoded excisionase (Xis) protein plays an essential role in regulating the directionality of recombination, dramatically stimulating phage excision while simultaneously inhibiting viral integration (Bushman *et al.*, 1984; Thompson *et al.*, 1987; Moitoso de Vargas & Landy, 1991; Franz & Landy, 1995). Xis cooperatively binds to two sites within the P-arm of the phage (sites X_1 and X_2) and stimulates excision by stabilizing distorted structures within the excisive intasome. Specifically, gel-electrophoresis studies are consistent with Xis introducing bends of 45–90° when bound to individual sites X_1 and X_2; bends in excess of >140° have been observed when Xis is bound to both sites (Thompson & Landy, 1988). In addition to its important architectural role, Xis also cooperatively recruits the phage-encoded Int and host-encoded Fis proteins (Bushman *et al.*, 1984; Thompson *et al.*, 1987). The combination of DNA bending and protein–protein interactions is believed to position the catalytic domain of Int appropriately for target capture and catalysis within the fully assembled excisive intasome.

The Xis protein is the archetypal member of a large superfamily of recombination directionality factors (RDFs; Lewis & Hatfull, 2001). At present, the only structural information for any RDF comes from the recently determined NMR structure of Xis solved in the absence of DNA (Sam *et al.*, 2002). Xis adopts an unusual 'winged'-helix DNA-binding fold and is postulated to distort DNA through both major- and minor-groove interactions. In addition, the C-terminal tail of Xis (residues 56–72), which is required for cooperative interactions with Int (Numrych *et al.*, 1992; Cho *et al.*, 2002; Sarkar *et al.*, 2002), is unstructured in the absence of Int and DNA (Sam *et al.*, 2002). However, this work left unresolved the molecular basis by which Xis recognizes and dramatically distorts DNA, or how it cooperatively recruits Int and Fis during phage recombination. As a step towards answering these remaining questions, we have obtained crystals and performed a preliminary X-ray crystallographic analysis of Xis in complex with its cognate DNA-binding site.

2. Materials and methods

2.1. Purification of $^{1-55}Xis^{C28S}$ and its cognate DNA-binding site

The DNA-binding domain of the excisionase protein containing a single amino-acid mutation ($^{1-55}Xis^{C28S}$; residues 1–55 of excisionase with a Cys→Ser mutation at position 28) was expressed and purified for crystallization trials. This protein is biologically active and was

© 2003 International Union of Crystallography
Printed in Denmark – all rights reserved

made based on two important findings: (i) only the N-terminal 55 residues of Xis are required for DNA binding (Numrych *et al.*, 1992; Sam *et al.*, 2002) and (ii) at high concentrations of Xis, artifactual disulfide-linked dimers of the protein are formed through its single cysteine residue (data not shown). The plasmid pRJ1709 (Sam *et al.*, 2002) encoding $^{1–55}$Xis^{C28S} was transformed into *Escherichia coli* strain BL21(DE3) (Novagen). Cells were then grown in 6 l of M9 minimal media containing ^{15}N-enriched ammonium chloride as the sole nitrogen source to an OD_{600} of 0.3. The cells were then induced with 1 m*M* IPTG for a period of 1 h, harvested, lysed and the Xis protein precipitated from the clear cell extract by the addition of ammonium sulfate to 45% saturation (273 K). The ammonium sulfate pellets were resuspended in 3 ml of buffer (2 *M* urea, 0.3 *M* NaCl and 50 m*M* $NaPO_4$ pH 6.0), solubilized and applied to a Sephacryl-S100 (Pharmacia Biotechnology) size-exclusion column. Fractions containing $^{1–55}$Xis^{C28S} were pooled and dialyzed into a low-salt buffer (50 m*M* NaCl and 50 m*M* NaOAc pH 5.5) and applied to a Resource-S cation-exchange column (Pharmacia Biotech). $^{1–55}$Xis^{C28S} was then eluted with a linear gradient (0.05–1 *M*) of NaCl. The pooled fractions from the Resource-S column were free from contaminants when analyzed by SDS–PAGE. NMR spectra of uniformly ^{15}N-enriched $^{1–55}$Xis^{C28S} were also recorded to assess the purity and structural integrity of the protein prior to crystallization trials.

DNA oligonucleotides used for crystal screening were purchased from Biosource International and were subjected to a two-step purification procedure. First, each individual single-stranded oligonucleotide was purified by application to a 1 ml MonoQ column under denaturing conditions (6 *M* urea and 50 m*M* Tris–HCl pH 7.0) using a linear salt gradient (0.15–0.45 *M* NaCl). The appropriate ssDNA oligonucleotides were then annealed by heating and slow cooling and the resulting dsDNA was separated from excess ssDNA by re-application to the MonoQ column (0.15–0.45 *M* NaCl gradient in 50 m*M* Tris pH 7.0 and 1 m*M* EDTA).

2.2. Complex formation

A series of $^{1–55}$Xis^{C28S}–DNA complexes were screened for crystal growth using a variety of oligonucleotides that all contained the nucleotide sequence of the X_2 binding site (5′-TATGTAGTCTGTT). However, these screened oligonuclotides differed in overall length (by the addition of one or two base pairs flanking the X_2 binding site). Furthermore, these oligonucleotides were either blunt-ended or contained an A or a T base overhang, a technique commonly used to crystallize protein–DNA complexes. Complexes were formed under high-salt conditions (200 m*M* NaCl and 50 m*M* NaOAc pH 5.0) with the DNA and protein components at 100 µ*M*. The complexes were then buffer-exchanged to remove NaCl (using a Centriprep-YM3; Amicon) and concentrated to approximately 12 mg ml^{-1} (using a Microcon-YM3; Millipore). Before crystal screening, an NMR ^{1}H–^{15}N HSQC spectrum was recorded to ensure that a distinct and specific complex had formed. It is worth noting that although the NMR spectra of the $^{1–55}$Xis^{C28S}–DNA complex suggest that it is monodisperse (as judged by resolved amide cross-peaks in the HSQC spectrum), nearly one third of the cross-peaks are broadened, suggesting that a high-resolution structure determination by NMR would be problematic, if not impossible.

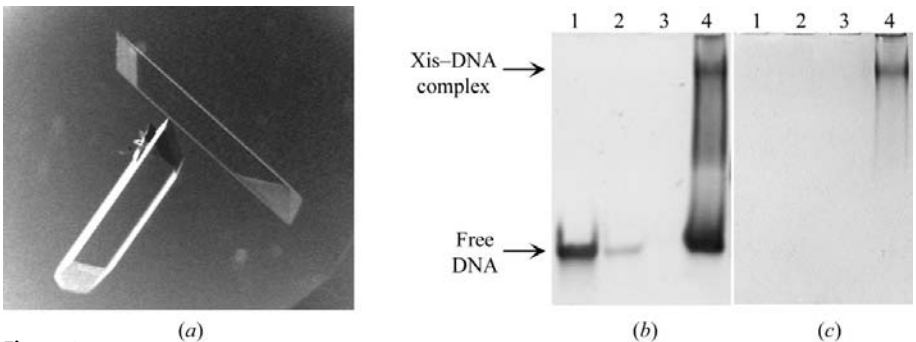

Figure 1
(*a*) Typical crystals of the $^{1–55}$Xis^{C28S}–DNA complex grown in 1 *M* NaOAc, 0.1 *M* imidazole pH 6.5 and 10 mg ml^{-1} complex. The crystal grew to dimensions of 0.5 × 0.15 × 0.1 mm in approximately one month. (*b*) 15% polyacrylamide native gel stained to selectively visualize only the DNA (SYBR-Gold nucleic acid gel stain; Molecular Probes). Lane 1, control 15-mer duplex DNA (1 µg); lane 2, control 15-mer duplex DNA (0.1 µg); lane 3, solution recovered from the crystal-washing procedure; lane 4, DNA in dissolved crystal. (*c*) The same gel as shown in (*b*), but stained for protein with Coomassie blue. Comparing the retarded band in lane 4, Figs. 1(*b*) and 1(*c*) show that the crystal does in fact contain the $^{1–55}$Xis^{C28S}–DNA complex.

3. Results

3.1. Crystallization of $^{1–55}$Xis^{C28S}–DNA complex

Hampton Research Crystal Screen kits I and II were used to determine the crystallization conditions. Co-crystals were screened at 291 K using the hanging-drop vapor-diffusion method, in which 1 µl of the $^{1–55}$Xis^{C28S}–DNA complex solution was mixed with 1 µl of the well solution and allowed to equilibrate against 1 ml of the well solution. Reproducible high-quality crystals were observed with $^{1–55}$Xis^{C28S}–DNA complexes containing the blunt-ended sequence 5′-CTATGTAGTCTGTTG/5′-CAACAGACTACATAG. The Hampton kits resulted in several potential crystallization leads and each lead was further investigated to determine the optimal conditions for crystal growth. Each lead was systematically screened by varying every component within the crystallization condition, including the concentration of the complex. The best crystals diffracted beyond 1.5 Å and were grown using 1 *M* NaOAc, 0.1 *M* imidazole pH 6.5 and 10 mg ml^{-1} protein–DNA complex. Nucleation of crystal seeds was generally observed within the first week and crystals typically grew to 0.50 × 0.15 × 0.10 mm in approximately one month (Fig. 1*a*). To ensure that these crystals consist of both components of the complex, single crystals were isolated, washed and analyzed using a 15% native polyacrylamide gel (Figs. 1*b* and 1*c*). The gel analysis revealed a slower migrating band that stained for both DNA and protein (Figs. 1*b* and 1*c*; lane 4), thus confirming the presence of the $^{1–55}$Xis^{C28S}–DNA complex in the crystals.

3.2. Data collection and processing

Crystals were mounted in a nylon loop and cryoprotected by the addition of 25% glycerol to the mother liquor. Crystals were cryocooled under a nitrogen stream at home and transferred to the Brookhaven National Synchrotron Light Source (NSLS) Laboratory, where a complete native data set was collected at beamline X8C. X-ray diffraction data were collected at a crystal-to-detector distance of 100 mm with a 1° oscillation angle per image. A typical oscillation image showing Bragg reflections extending beyond 1.5 Å is shown in Fig. 2.

Diffraction data were processed with the *HKL* package (Otwinowski & Minor, 1997). The reflection intensities were integrated with the program *DENZO* and then merged and scaled using the program *SCALE-*

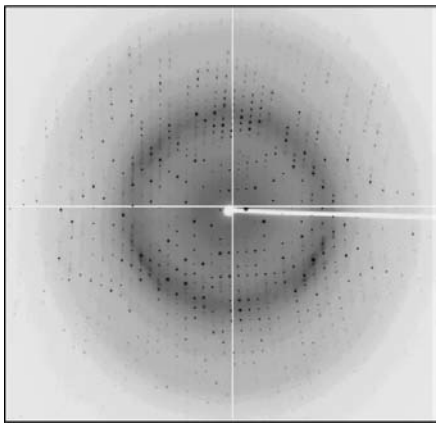

Figure 2
A typical 1° oscillation image of $^{1-55}$Xis^{C28S}–DNA complex, showing Bragg reflections extending beyond 1.5 Å resolution.

PACK. These crystals belong to the *C*-centered space group *C*2, with unit-cell parameters a = 80.2, b = 72.7, c = 38.8 Å, β = 104.1°. The processed and scaled data is 93% complete, with a redundancy of 3.8 and an overall R_{sym} of 5.0% (37% in the highest resolution shell, 1.55–1.5 Å; see Table 1 for complete statistics). Based on the Laue symmetry, this particular space group and unit-cell parameters, the calculated Matthews coefficient V_M (Matthews, 1968) is 3.43 Å^3 Da^{-1} for one $^{1-55}$Xis^{C28S}–DNA complex per asymmetric unit. This corresponds to an estimated solvent content of 64%, which is within the typical range observed for protein and/or DNA macromolecules.

Table 1
X-ray crystallographic parameters and data-collection statistics.

Values in parentheses are for the highest resolution shell.

Beamline	NSLS-X8C
Wavelength (Å)	1.10
Space group	*C*2
Unit-cell parameters (Å, °)	a = 80.2, b = 72.7, c = 38.8, β = 104.1
Matthews coefficient (Å^3 Da^{-1})	3.34
Solvent content (%)	64
Resolution (Å)	100–1.50 (1.55–1.50)
No. observations	122089 (11259)
No. unique reflections	32190 (3131)
Completeness (%)	93.1 (90.7)
R_{sym}†	0.050 (0.377)
$\langle I/\sigma(I)\rangle$‡	19.8 (3.2)

† $R_{sym} = \sum_{hkl}\sum_i |I_i(hkl) - \langle I(hkl)\rangle| / \sum_{hkl}\sum_i I_i(hkl)$, where I_i is the ith measurement of reflection $I(hkl)$. ‡ $\langle I/\sigma(I)\rangle$ is the the mean reflection intensity divided by the estimated error of the intensity.

Attempts to solve the structure of the protein–DNA complex by molecular replacement using the solution structure of the $^{1-55}$Xis^{C28S} protein (Sam *et al.*, 2002) as a search model and the programs *EPMR* (Kissinger *et al.*, 1999) and *AMoRe* (Navaza, 1994) have proven unsuccessful. At present, we are attempting to obtain phases by growing crystals with 5-iodouracil substituted for thymines within the DNA, so as to enable the application of multiple isomorphous replacement augmented with anomalous scattering (MIRAS) methods. Crystals with 5-iodouracil at two unique positions have been obtained and are expected to be helpful if not sufficient to determine the structure of the $^{1-55}$Xis^{C28S}–DNA complex.

The authors wish to thank Dr Michael Sawaya for his help in collecting the X-ray data and continued support. This work was supported by National Institutes of Health grant GM57487 to RTC.

References

Azaro, M. A. & Landy, A. (2002). *Mobile DNA II*, edited by N. L. Craig, R. Craigie, M. Gellert & A. M. Lambowitz, pp. 118–148. Washington, DC: ASM Press.
Bushman, W., Yin, S., Thio, L. L. & Landy, A. (1984). *Cell*, **39**, 699–706.
Cho, E. H., Gumport, R. I. & Gardner, J. F. (2002). *J. Bacteriol.* **184**, 5200–5203.
Franz, B. & Landy, A. (1995). *EMBO J.* **14**, 397–406.
Kissinger, C. R., Gehlhaar, D. K. & Fogel, D. B. (1999). *Acta Cryst.* D**55**, 484–491.
Lewis, J. A. & Hatfull, G. F. (2001). *Nucleic Acids Res.* **29**, 2205–2216.
Matthews, B. W. (1968). *J. Mol. Biol.* **33**, 491–497.
Moitoso de Vargas, L. & Landy, A. (1991). *Proc. Natl Acad. Sci. USA*, **88**, 588–592.
Navaza, J. (1994). *Acta Cryst.* A**50**, 157–163.
Numrych, T. E., Gumport, R. I. & Gardner, J. F. (1992). *EMBO J.* **11**, 3797–3806.
Otwinowski, Z. & Minor, W. (1997). *Methods Enzymol.* **276**, 307–326.
Sam, M. D., Papagiannis, C., Connolly, K. M., Corselli, L., Iwahara, J., Lee, J., Phillips, M., Wojciak, J. M., Johnson, R. C. & Clubb, R. T. (2002). *J. Mol. Biol.* **324**, 791–805.
Sarkar, D., Azaro, M. A., Aihara, H., Papagiannis, C. V., Tirumalai, R., Nunes-Duby, S. E., Johnson, R. C., Ellenberger, T. & Landy, A. (2002). *J. Mol. Biol.* **324**, 775–789.
Thompson, J. F. & Landy, A. (1988). *Nucleic Acids Res.* **16**, 9687–9705.
Thompson, J. F., Moitoso de Vargas, L., Koch, C., Kahmann, R. & Landy, A. (1987). *Cell*, **50**, 901–908.